# Computer-Aided Synthesis of Lumped Lossy Matching Networks for Monolithic Microwave Integrated Circuits (MMIC's)

LOUIS C. T. LIU, MEMBER, IEEE, AND WALTER H. KU, MEMBER, IEEE

*Abstract*—A systematic computer-aided synthesis (CAS) technique of lumped lossy matching networks is presented in this paper. This exact synthesis procedure can take arbitrary finite quality factor $Q$ for each lumped element in the matching network and therefore facilitate the circuit design for monolithic microwave integrated circuits (MMIC's) where the loss of the passive elements is too large to be neglected. The gain–bandwidth limitations of some useful lumped lossy matching networks are discussed in detail and are summarized in a set of gain–bandwidth constraint plots. An interactive computer program LUMSYN is developed to solve this lumped lossy synthesis problem. LUMSYN is a general-purpose CAS program which can be used by microwave circuit designers with limited background in network synthesis to carry out low-noise and power amplifier designs in MMIC's. Finally, a design example of broad-band monolithic microwave low-noise amplifier using a state-of-the-art low-noise submicron gate-length GaAs MESFET is presented to illustrate the computer-aided synthesis of MMIC amplifiers.

## I. Introduction

THE ADVANCES IN GaAs material development and wafer processing achieved in the past few years have made the monolithic microwave integrated circuits (MMIC's) practical [1], [2]. These integrated circuits have potential applications in the low-cost transmit–receive modules for phased array radars and in the $X$-band receivers for satellite direct-broadcast television. This paper is intended to provide a systematic computer-aided synthesis and design (CAS/CAD) procedure, which forms part of the basic technology for the development of MMIC's.

In the design of MMIC's, the matching networks consist of lumped reactive elements and/or transmission-line elements. Lumped elements are often essential since they occupy less GaAs chip area and have broader bandwidth capability. Unfortunately, the lumped elements fabricated on the semi-insulating GaAs substrates have losses which are too large to be neglected. Due to the lack of a lossy synthesis technique, most circuit designers will first synthesize a lossless matching network and then simply add loss elements to each lumped circuit component. Since the loss elements added have different effects to the transducer power gain at different frequencies, the gain response will be out of control. The development of a lumped lossy matching network synthesis technique is therefore very desirable for MMIC's.

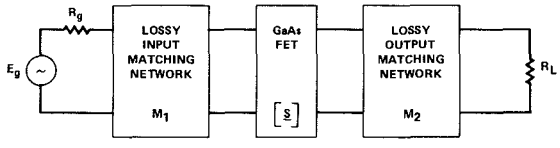


Fig. 1. Block diagram of a single-stage GaAs FET amplifier.

The exact synthesis of lumped networks with lossy elements has been an open problem with long standing for the general case of arbitrary nonuniform dissipation. Using both analytical and CAS techniques, we have solved the lossy synthesis problem for the case of unequal inductor and capacitor losses with arbitrary circuit topology and realizable gain functions. This new result is directly applicable to the synthesis of the matching networks for MMIC's. Presently, the new theory we have developed does not take the parasitic reactances of the lossy circuit elements into account, and CAD and optimization techniques must be used to "fine-tune" the synthesized amplifier response, thus modifying the element values of the actual lossy $L$'s and $C$'s of the matching network. Our preliminary study indicates that the integrated analytical and CAD approach we have used for the successful synthesis of lossy matching networks for MMIC's can also be extended to the more general problem.

## II. Exact Synthesis of Lumped Lossy Matching Networks

In MMIC's, the matching network should be synthesized to provide a desired impedance match between the output of one stage and the input of the next stage. For example, Fig. 1 is the block diagram of a basic single-stage GaAs MESFET amplifier. The matching networks $M_1$ and $M_2$ should provide a good impedance match which includes

Manuscript received August 11, 1983; revised December 29, 1983. This work was supported in part by the Joint Services Electronics Program at Cornell University under AFOSR Contract F49620-81-C-0082, monitored by Dr. G. Witt.

L. C. T. Liu is with the Torrance Research Center, Hughes Aircraft Co., Torrance, CA, 90509.

W. H. Ku is with the School of Electrical Engineering and National Submicron Facility, Cornell University, currently on sabbatical leave as Distinguished Visiting Professor at the Department of Electrical Engineering and Computer Sciences, University of California, San Diego, La Jolla, CA 92093.

0018-9480/84/0300-0282$01.00 ©1984 IEEE


Fig. 2. Simplified equivalent circuit for lumped reactive elements.

the compensation of the gain roll-off of the FET between $R_g$ and the input of the FET, and the output of the FET and $R_L$, respectively. While trying to match the input or output of the FET, simplified models for the FET are usually used to avoid complicated network synthesis. For instance, the input equivalent circuit of a lumped GaAs FET model is a series capacitor terminated with a resistor, and the output equivalent circuit is a parallel capacitor terminated with a resistor. The matching networks will then absorb the reactances of these simplified equivalent circuits while providing the specific gain response.

In order to synthesize a matching network, a realizable gain function should be obtained first. In this paper, only the lumped lossy matching network is considered. The transducer power gain function of a lumped lossy matching network must contain the lossy element which accompanies each lossy reactance of the matching network. As shown in Fig. 2, the simplified model of a monolithic lumped inductor is considered as an ideal inductor in series with a resistor $r$, which is then specified in terms of the quality factor $Q_L$ defined as

$$r = \frac{\omega_0 L}{Q_L} \tag{1}$$

where $L$ is the value of the ideal lossless inductor and $\omega_0$ is the frequency at which the $Q_L$ is defined. The impedance of the lossy inductor is then given by

$$Z_L = r + sL = \frac{\omega_0 L}{Q_L} + sL = (s + \alpha_L)L \tag{2}$$

where $\alpha_L = \omega_0/Q_L$ is the inductor loss or dissipation factor. Similarly, a simplified model of a lossy capacitor is considered as an ideal lossless capacitor $C$ in parallel with a resistor with conductance $g$. If this conductance is specified in terms of the quality factor $Q_c$ as

$$g = \frac{\omega_0 C}{Q_c} \tag{3}$$

then the admittance of the lossy capacitor is given by

$$Y_c = g + sC = \frac{\omega_0 C}{Q_c} + sC = (s + \alpha_c)C \tag{4}$$

where $\alpha_c \doteq \omega_0/Q_c$ is the capacitor loss factor. Consider the appropriate impedance and admittance presented in (2) and (4). It is clear that the basic transformation of variable from $s$ to $(s + \alpha)$ will incorporate the losses of the $L$'s and $C$'s, and the gain function of a lossy matching network is

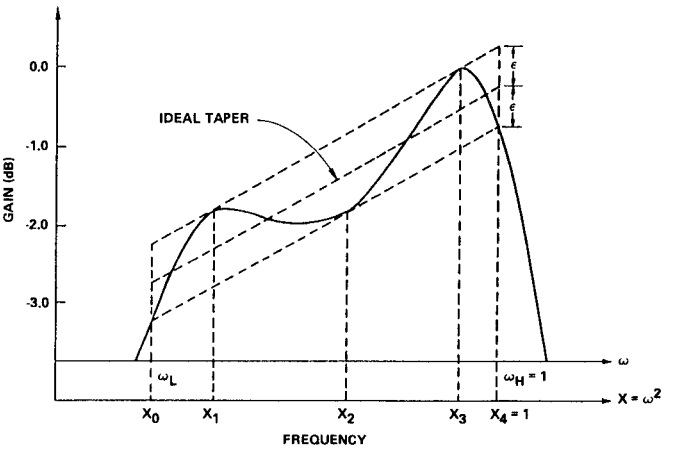


Fig. 3. Ideal taper and its equiripple approximation of a matching network.

given by

$$G_M(\omega^2) = \frac{k(\omega^2 + \alpha_1^2)(\omega^2 + \alpha_2^2)\cdots(\omega^2 + \alpha_m^2)}{p_n(\omega^2)} = \frac{k\prod_{j=1}^{m}(x + \alpha_j^2)}{p_n(x)} \tag{5}$$

where

$x = \omega^2$,
$m$ = number of high-pass elements,
$P_n(x)$ = an $n$th order polynomial which will be derived to provide an equiripple or maximally-flat gain function,
$k$ = gain constant,
$\alpha_j$ = loss factor of $j$th high-pass element.

The equiripple error gain function provides a better initial overall gain response of the amplifier. In addition, it is much more flexible in the reactive element absorption and impedance ratio transformation. Therefore, in the following discussion only the equiripple error gain function will be considered. It is the task now to derive the polynomial $P_n(x)$ such that the gain function will be realizable and meet certain requirements. The same approach used by Petersen [3] to derive a lossless equiripple gain function is adopted here.

Fig. 3 shows a typical tapered equiripple gain function with $n = 4$, which is required for certain matching networks to provide gain matching from one end to the other. In the figure, $\omega_H$ is normalized to 1 rad/s, $\epsilon$ is the size of the maximum error in decibels, and $x_0$, $x_1$, $x_2$, $x_3$, and $x_4$ are called critical points since the approximate gain function has maximum error at those points. To solve for the general $n$th-order gain function, the value of the $n-1$ critical points (since $x_0$ and $x_n$ are known) and the $n$ coefficients of $P_n(x)$ have to be solved. Let $G_M(x)$ and $\hat{f}(x)$ represent the equiripple approximation and ideal gain function (e.g., the center dotted line in Fig. 3), respectively; then the error function $E(x)$ on a log–log scale can be

written as

$$E(x) = \ln[G_M(x)] - \ln[\hat{f}(x)]. \tag{6}$$

If the passband is normalized to the interval $[x_0, 1]$, as shown in Fig. 3, the equiripple conditions can be written as

$$E(x_i) = (-1)^i \epsilon, \qquad i = 0,1,\cdots,n \tag{7}$$

$$\left.\frac{dE(x)}{dx}\right|_{x=x_i} = 0, \qquad i = 0,1,\cdots,n \tag{8}$$

where $x_0 < x_1 < \cdots < x_n$ are the points of maximum error. The ideal tapered gain function is given by

$$\hat{f}(x) = x^{\hat{\alpha}} \tag{9a}$$

where

$$\hat{\alpha} = \frac{\text{SLOPE(dB/OCTAVE)}}{20\log_{10}2}. \tag{9b}$$

Define

$$f(x) = \frac{1}{\hat{f}(x)} = x^{-\hat{\alpha}} \tag{10}$$

and

$$B^i = \begin{cases} e^{\epsilon}, & i \text{ even} \\ e^{-\epsilon}, & i \text{ odd} \end{cases}. \tag{11}$$

From (6) and (7), it can be derived that

$$\ln\left[\frac{\prod_{j=1}^{m}\left(x_i + \alpha_j^2\right)}{p_n(x_i)}\right] + \ln[f(x_i)] + \ln B_i = 0, \qquad i = 0,1,\cdots,n. \tag{12}$$

Since the gain constant $k$ only changes the gain level and not the shape of the gain response, it can be set to 1 at this moment. Then from (12), it can be seen that

$$B_i \prod_{j=1}^{m}\left(x_i + \alpha_j^2\right) f(x_i) = P_n(\underset{\sim}{a}, x_i), \qquad i = 0,1,\cdots,n \tag{13a}$$

where

$$P_n(\underset{\sim}{a}, x_i) = P_n(x_i) = a_0 + a_1 x_i + \cdots a_n x_i^n. \tag{13b}$$

Invoking (13), the first equiripple condition, or (7), becomes

$$\underset{\sim}{a} = \boldsymbol{X}^{-1}\underset{\sim}{R}(\underset{\sim}{x}) \tag{14a}$$

where

$$\underset{\sim}{a} = [a_0\ a_1 \cdots a_n]^T \tag{14b}$$

$$\underset{\sim}{x} = [x_0\ x_1 \cdots x_n]^T \tag{14c}$$

$$\boldsymbol{X} = \begin{bmatrix} 1 & x_0 & x_0^2 & \cdots & x_0^n \\ 1 & x_1 & x_1^2 & \cdots & x_1^n \\ \vdots & & & & \vdots \\ 1 & x_n & x_n^2 & \cdots & x_n^n \end{bmatrix} \tag{14d}$$

$$\underset{\sim}{R}(\underset{\sim}{x}) = \begin{bmatrix} B_0 \prod_{j=1}^{m}\left(x_0 + \alpha_j^2\right) f(x_0) \\ B_1 \prod_{j=1}^{m}\left(x_1 + \alpha_j^2\right) f(x_1) \\ \vdots \\ B_n \prod_{j=1}^{m}\left(x_n + \alpha_j^2\right) f(x_n) \end{bmatrix}. \tag{14e}$$

Let $F(x_i)$ be the numerator of $E'(x_i)$, where the prime denotes the differentiation with respect to $x$. Then from (6) and the second equiripple condition, or (8), it can be shown that

$$F(x_i) = P_n(x_i)\left[\sum_{j=1}^{m}\frac{1}{x_i + \alpha_j^2} f(x_i) + f'(x_i)\right] - f(x_i)P_n'(x_i) = 0, \qquad i = 1,2,\cdots,(n-1). \tag{15}$$

Equations (14) and (15) are now the equivalent conditions for the equiripple error gain function. Newton's iteration method [4] can be used to solve for $x_i$'s by inserting (14) into (15). The iteration formula in Newton's method is given by

$$\underset{\sim}{x}^{(k+1)} = \underset{\sim}{x}^{(k)} - \beta \boldsymbol{J}^{-1}\left(\underset{\sim}{x}^{(k)}\right)\underset{\sim}{F}\left(\underset{\sim}{x}^{(k)}\right) \tag{16a}$$

where

$$\beta = 1 \tag{16b}$$

$$F(x^{(k)}) = \left[F\left(x_1^{(k)}\right)\ F\left(x_2^{(k)}\right)\cdots F\left(x_{n-1}^{(k)}\right)\right]^T \tag{16c}$$

$$\boldsymbol{J}\left(\underset{\sim}{x}^{(k)}\right) = \left.\frac{\partial F(x)}{\partial \underset{\sim}{x}}\right|_{\underset{\sim}{x}=\underset{\sim}{x}^{(k)}} = \begin{bmatrix} \frac{\partial F(x_1)}{\partial x_1} & \frac{\partial F(x_1)}{\partial x_2} & \cdots & \frac{\partial F(x_1)}{\partial x_{n-1}} \\ \frac{\partial F(x_2)}{\partial x_1} & \frac{\partial F(x_2)}{\partial x_2} & \cdots & \frac{\partial F(x_2)}{\partial x_{n-1}} \\ \vdots & \vdots & & \vdots \\ \frac{\partial F(x_{n-1})}{\partial x_1} & \frac{\partial F(x_{n-1})}{\partial x_2} & \cdots & \frac{\partial F(x_{n-1})}{\partial x_{n-1}} \end{bmatrix}_{\underset{\sim}{x}=\underset{\sim}{x}^{(k)}} \tag{16d}$$

and the superscripts $(k)$ refer to the number of iterations. In order to calculate the Jacobian matrix $\boldsymbol{J}$, (15) is expanded as

$$F(x_i)=\left(\sum_{j=0}^{n} a_j x_i^j\right)\left[\sum_{j=1}^{m}\frac{1}{x_i+\alpha_j^2}f(x_i)+f'(x_i)\right] - f(x_i)\left(\sum_{j=1}^{n} j a_j x_i^{j-1}\right). \quad (17)$$

Differentiating (17) with respect to one of the critical points, e.g., $x_l$, gives

$$\begin{aligned} J_{il}&=\frac{\partial F(x_i)}{\partial x_l}\\ &=\left\{P_n(x_i)\left[f''(x_i)+f'(x_i)\sum_{j=1}^{m}\frac{1}{x_i+\alpha_j^2} - f(x_i)\sum_{j=1}^{m}\frac{1}{\left(x_i+\alpha_j^2\right)^2}\right]\right.\\ &\quad\left.+P_n'(x_i)f(x_i)\sum_{j=1}^{m}\frac{1}{x_i+\alpha_j^2}-f(x)P_n''(x)\right\}\delta_{il}\\ &\quad+\left[\sum_{j=1}^{m}\frac{1}{x_i+\alpha_j^2}f(x_i)+f'(x_i)\right]\left(\sum_{j=0}^{m}\frac{\partial a_j}{\partial x_l}x_i^j\right)\\ &\quad-f(x_i)\left(\sum_{j=1}^{m} j\frac{\partial a_j}{\partial x_l}x_i^{j-1}\right) \end{aligned} \quad (18a)$$

where

$$\delta_{il}=\begin{cases}0, & i\neq l\\ 1, & i=l\end{cases}. \quad (18b)$$

Furthermore, $\partial a_j/\partial x_l$ can be calculated by differentiating (14) with respect to $x_l$ as

$$\frac{\partial \underset{\sim}{a}}{\partial \underset{\sim}{x}}=\boldsymbol{X}^{-1}\operatorname{diag}\left[\underset{\sim}{R}'(\underset{\sim}{x})-\underset{\sim}{P}_n(\underset{\sim}{x})\right] \quad (19a)$$

where

$$\frac{\partial \underset{\sim}{a}}{\partial \underset{\sim}{x}}=\begin{bmatrix}\frac{\partial a_0}{\partial x_0} & \frac{\partial a_0}{\partial x_1} & \cdots & \frac{\partial a_0}{\partial x_n}\\ \frac{\partial a_1}{\partial x_0} & \frac{\partial a_1}{\partial x_1} & \cdots & \frac{\partial a_1}{\partial x_n}\\ \vdots & \vdots & & \vdots\\ \frac{\partial a_n}{\partial x_0} & \frac{\partial a_n}{\partial x_1} & \cdots & \frac{\partial a_n}{\partial x_n}\end{bmatrix} \quad (19b)$$

and

$$\underset{\sim}{P}_n'(\underset{\sim}{x})=\left[P_n'(x_0)\ P_n'(x_1)\cdots P_n'(x_n)\right]. \quad (19c)$$

In order to start Newton's iteration, an initial vector $\underset{\sim}{x}^{(0)}$ has to be selected. One of the natural selections is the vector consisting of equi-distance points between $x_0$ and $x_{n'}$ or

$$\underset{\sim}{x}^{(0)}=\left[x_1^{(0)}x_2^{(0)}\cdots x_n^{(0)}\right]^T \quad (20a)$$

where

$$x_i^{(0)}=x_0+i\left[\frac{x_n-x_0}{n}\right]. \quad (20b)$$

The coefficient vector $\underset{\sim}{a}$ can then be calculated from (14). This result is used to calculate the next $\underset{\sim}{x}$ vector, or $\underset{\sim}{x}^{(1)}$, through (16). This procedure continues until $\underset{\sim}{x}^{(k+1)}$ converges to $\underset{\sim}{x}^{(k)}$. The final $\underset{\sim}{x}$ and $\underset{\sim}{a}$ will provide a gain function which meets the requirements specified earlier.

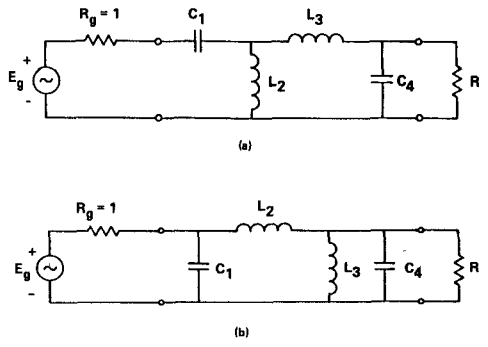


Fig. 4. Two possible topologies of the lumped lossy matching network. (a) $N=4$, $N_L=2$, $N_H=2$. (b) $N=4$, $N_L=3$, $N_H=1$.

After the shape of the gain response is determined, the gain constant $k$ can be used to adjust the gain level in order to satisfy other specifications, for example, the realizability of the gain function, gain–bandwidth limitation, impedance transformation ratio, and realizability of the element values. For a lossless matching network, the reflection coefficient can be calculated from $G_M(\omega^2)$ according to the following equations:

$$|S_{11}(j\omega)|^2=1-|S_{12}(j\omega)|^2=1-G_M(\omega^2) \quad (21)$$

and

$$|S_{11}(j\omega)|^2=S_{11}(s)S_{11}(-s)|_{s=j\omega}. \quad (22)$$

Therefore, the element value of the matching network can be obtained through the reflection coefficient or the input impedance function. However, in a lossy matching network synthesis, (21) is no longer valid, and there is no simple relation between $S_{21}(s)$ and $S_{11}(s)$. In order to derive the element values, the problem has to be solved by another method. The topology of the matching network can be determined first, and then the loss factor or quality factor $Q$ of each element is assigned according to practical considerations. The transducer power gain function $G_M(\omega^2)$ of the matching network can be calculated in terms of all the $L$'s, $C$'s, and $\alpha$'s associated with each element. By equating the coefficients of $P_n(\underset{\sim}{a}, x)$ and the gain constant obtained from both Newton's iteration and circuit calculation, $n+2$ nonlinear equations are formed (but since one of these can be absorbed by the others, only $n+1$ equations are needed). By solving these $n+1$ nonlinear equations, $n$ reactive element values and the load resistance $R$ can be obtained.

To illustrate the above procedure, an output matching network example is employed. Fig. 4(a) and (b) shows two possible topologies for input and output matching networks, respectively. The $S_{21}(s)$ of the output lossy matching network shown in Fig. 4(b) can be calculated as

$$S_{21}(s) = \frac{2RL_3(s+\alpha_3)}{b_0 + b_1 s + b_2 s^2 + b_3 s^3 + b_4 s^4} \tag{23a}$$

where

$$b_0 = (\alpha_1 C_1 + 1)(\alpha_2 L_2 R + \alpha_2\alpha_3\alpha_4 L_2 L_3 C_4 R + \alpha_2\alpha_3 L_2 L_3 + \alpha_3 L_3 R) + R + \alpha_3\alpha_4 L_3 C_4 R + \alpha_3 L_3 \tag{23b}$$

$$b_1 = C_1(\alpha_2 L_2 R + \alpha_2\alpha_3\alpha_4 L_2 L_3 C_4 + R + \alpha_2\alpha_3 L_2 L_3 + \alpha_3 L_3 R) + (\alpha_1 C_1 + 1)[L_2 R + L_2 L_3 C_4 R(\alpha_2\alpha_3 + \alpha_2\alpha_4 + \alpha_3\alpha_4) + L_2 L_3(\alpha_2 + \alpha_3) + L_3 R] + L_3 C_4 R(\alpha_3 + \alpha_4) + L_3 \tag{23c}$$

$$b_2 = C_1[L_2 R + L_2 L_3 C_4 R(\alpha_2\alpha_3 + \alpha_2\alpha_4 + \alpha_3\alpha_4) + L_2 L_3(\alpha_2 + \alpha_3) + RL_3] + (\alpha_1 C_1 + 1)[L_2 L_3 C_4 R(\alpha_2 + \alpha_3 + \alpha_4) + L_2 L_3] + L_3 C_4 R \tag{23d}$$

$$b_3 = (\alpha_1 C_1 + 1) L_2 L_3 C_4 R + C_1[L_2 L_3 C_4 R(\alpha_2 + \alpha_3 + \alpha_4) + L_2 L_3] \tag{23e}$$

$$b_4 = C_1 L_2 L_3 C_4 R. \tag{23f}$$

Therefore, the transducer power gain is given by

$$G_M(\omega^2) = \frac{4RL_3^2(\omega^2 + a_3^2)}{b_0^2 + (b_1^2 - 2b_0 b_2)\omega^2 + (b_2^2 + 2b_0 b_4 - 2b_2 - 2b_4)\omega^4 + (b_3^2 - 2b_2 b_4)\omega^6 + b_4^2\omega^8}. \tag{24}$$

By comparing the above equation with the lossy gain function (5), it can be shown that

$$\frac{k}{a_0} = \frac{4RL_3^2}{b_0^2} \tag{25a}$$

$$\frac{a_1}{a_0} = \frac{b_1^2 - 2b_0 b_1}{b_0^2} \tag{25b}$$

$$\frac{a_2}{a_0} = \frac{b_2^2 + 2b_0 b_4 - 2b_1 b_3}{b_0^2} \tag{25c}$$

$$\frac{a_3}{a_0} = \frac{b_3^2 - 2b_2 b_4}{b_0^2} \tag{25d}$$

$$\frac{a_4}{a_0} = \frac{b_4^2}{b_0^2}. \tag{25e}$$

By solving the above set of nonlinear equations, the element values for $C_1$, $L_2$, $L_3$, $L_4$, and $R$ can be obtained.

The nonlinear equation set (25) can be solved most easily by the help of a digital computer. Either Brown's derivative-free method [5] or Marquardt's algorithm [6] can be used for this purpose. Both methods need a good initial guess to start the iteration for a solution. The element values generated from a lossless matching network synthesis procedure turn out to be a natural and good choice. The reason is that the lossy matching network desired should have exactly the same shape as that of the lossless one, only the gain level should be lower. Consequently, a solution from lossless matching network synthesis can be used as an initial guess for the lossy matching network with certain gain reduction (e.g., 0.5 dB) added to the gain function to compensate for the gain reduction due to the losses in the matching network. The result turns out to be very good as will be shown in the next section. Once a set of solutions for the lossy matching network is obtained, it can serve as an initial guess for other lossy matching networks with similar gain slope, gain reduction, or gain ripple. Since the gain constant $k$ changes only the gain level and not the general shape of the gain response, it will be very convenient to solve a specified gain function first and then to change just the $k$ to obtain a set of matching networks with different gain levels. This is the way the matching network tables are generated in the next section.

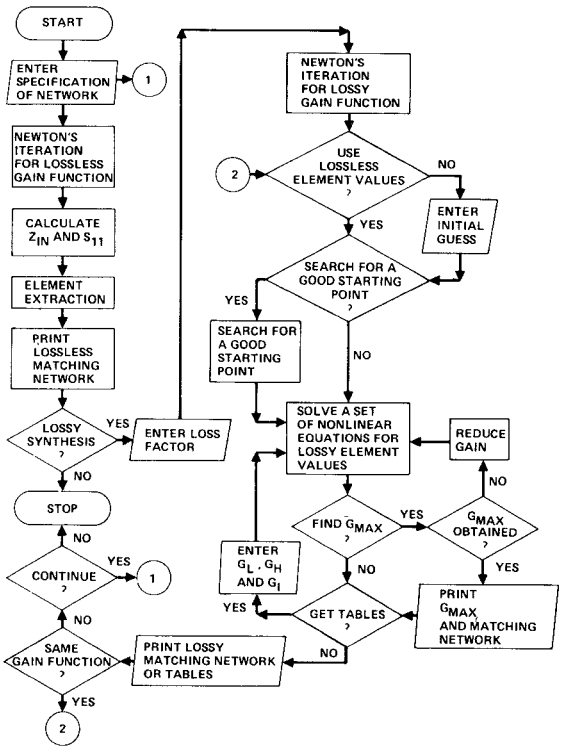


Fig. 5. Simplified flow chart of LUMSYN program.

## III. LUMSYN Program

An interactive program called LUMSYN written in FORTRAN has been developed to solve the lumped lossy synthesis formulation discussed in the previous section. It is the hope of the authors that people who do not specialize in network synthesis can still use it as a design tool for MMIC design. Therefore, a considerable amount of time and effort has been put into the program design to make it easier to understand and use.

Fig. 5 shows a simplified flow chart of the LUMSYN program. In this flow chart, it can be seen that after the

user specifies the gain function desired, the program will solve for a lossless gain function and the element values of the matching network which provides the desired gain response. If the user wishes to synthesize a lossy matching network, the loss factor of each reactive element has to be specified and a lossy gain function will then be obtained by Newton's method. The user now can use the element values of the lossless matching network as an initial guess, or enter his own initial guess, or ask the program to search for a good initial guess, to solve the element values of the lossy matching network. The search routine will systematically search an $n$-dimensional region for different initial guesses and then compare their function values and pick the best initial guess. In this search routine, Aird and Rice's systematic algorithm [7] has been adopted. After the element values of the lossy matching network are acquired, an iteration method is used to obtain the maximum gain $G_{\max}$ under certain gain specifications such as gain slope and gain ripple by decreasing the gain reduction step by step. As shown in Fig. 5, another feature of LUMSYN is to get a set of element value tables with the same general gain response shape but different gain reductions. The user can then keep the same gain function and vary the gain reduction, or solve for another gain function, or terminate the running section by entering the appropriate commands.

One thing that might be interesting to the circuit designer is the uniqueness of the solution. It has been proved that the equiripple gain function is unique under a certain frequency bandwidth, gain slope, and gain ripple [3]. However, the element values with specified loss factors are obtained by solving a set of nonlinear equations. Theoretically, this kind of solution cannot be proved to be unique. Fortunately, a systematic search routine is available, and it is used to find all the possible solutions. It is found that with lots of different initial guesses, the entire set of solutions converge to $2^{(n/2)-1}$ practical solutions, where $n$ is the order of the matching network. These $2^{(n/2)-1}$ solutions correspond to the $2^{(n/2)-1}$ different distributions of the zeros of the reflection coefficient, or $S_{11}(s)$, in the lossless matching network synthesis [3]. It can be concluded, therefore, that the lossy matching network solved by the above method is unique. This conclusion will be demonstrated further in the next section when the gain–bandwidth limitations are discussed.

## IV. Gain–Bandwidth Limitations for Lossy Matching Networks

The general gain–bandwidth limitation of the lossless matching networks was introduced by Bode [8] in 1945, and was extended by Fano [9] and Youla [10]. Applying this theory to the typical simplified FET model, two integral inequalities can be obtained. Ku and Petersen [11] used ideal tapered gain functions to derive the optimum gain–bandwidth limitations which yield an upper bound of the capability of reactive element absorption under the specific gain slope, gain reduction, and bandwidth. Therefore, before a matching network is synthesized for a certain FET, the optimum gain–bandwidth limitations of the FET simplified model can be checked first to determine the appropriate gain slope, gain reduction, and bandwidth. For the actual design of the GaAs FET amplifiers, the gain–bandwidth limitation of practical gain functions must be employed. The practical gain–bandwidth constraint plots for a lossy input and output matching network are shown in Fig. 6(a) and (b), respectively.

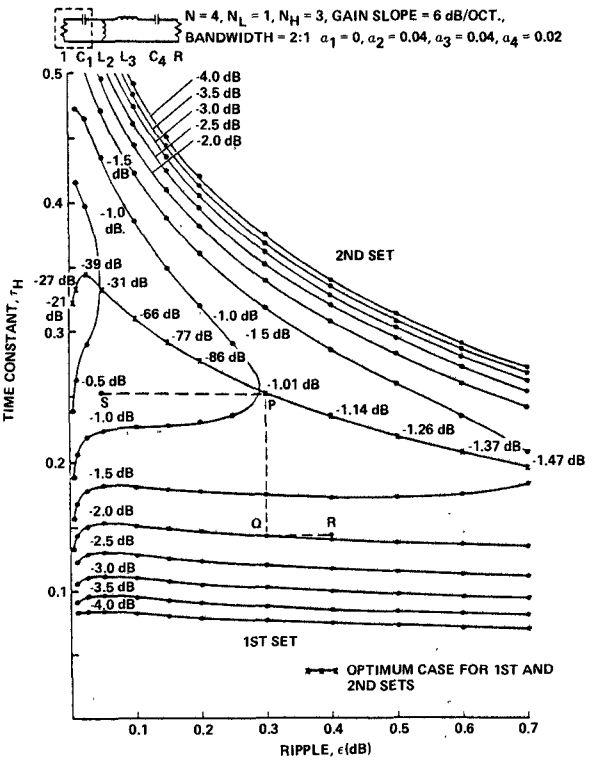


Fig. 6. (a) Gain–bandwidth constraint for lumped lossy input matching networks. (b) Gain–bandwidth constraint for lumped lossy output matching networks.

For a lossy matching network with some prescribed gain slope and gain ripple, there is a minimum gain reduction which has to be put into the gain function in order to obtain a realizable network. This is the minimum gain reduction introduced by the element losses in the matching network, and the gain level in this situation is called $G_{max}$. Any matching network with a gain level lower than $G_{max}$ is realizable while any matching network with a gain level higher than $G_{max}$ is unrealizable. In addition, this $G_{max}$ is a function of both gain slope and gain ripple for a certain topology of a matching network. Due to the nonlinearity of the lossy matching network, there is no analytical method to calculate the $G_{max}$. As a result, an iteration method is employed to determine the $G_{max}$. The gain–bandwidth limitation curves with $G_{max}$ are plotted in Fig. 6 as the optimum cases. These optimum cases correspond to the 0-dB gain reduction states in the lossless matching network. Each of these states has a zero of the reflection coefficients on the $j\omega$-axis. The other zeros may be either in the left-half plane (LHP) or in the right-half plane (RHP), or in a mixed distribution form. Each different distribution of zeros has a different $G_{max}$, and hence generates a new set of optimum curves in the gain–bandwidth constraint plots. For the $n = 4$ case, one set of complex conjugated zeros is on the $j\omega$-axis and another set of zeros can be either in the LHP or RHP in the complex $S$-plane. Therefore, two optimum curves are generated as shown in Fig. 6. Beginning with an optimum case, when some gain reduction is added to the matching network, the zeros on the $j\omega$-axis will move away from the $j\omega$-axis. Since there are two directions that the zeros can take, i.e., move into LHP or RHP, there are two solutions with the same gain response but different gain–bandwidth constraints. The result is that there are two sets of curves with the same gain reduction as shown in Fig. 6(a) and (b). The gain–bandwidth constraint curves with a certain gain reduction have to merge to the optimum curves; therefore, these will have different shapes than those of the lossless case.

Two possible input and output matching networks for a GaAs MESFET are shown in Fig. 6(a) and (b), respectively. In the figure, $N$ is the order of the matching network, $N_L$ and $N_H$ are the number of the low-pass and high-pass elements, respectively. The loss factors, $\alpha_i$'s, for inductor and capacitor are defined in (2) and (4), with their values being normalized at $\omega_H = 1$. The gain reduction at the optimum case is the maximum gain that the matching network can have under certain gain slope and ripple, and was defined as $G_{max}$. The reactance absorption capability will increase with higher gain reduction. The first set of curves in Fig. 6(a) illustrate this property if the element $C_1$ is considered as the reactive element to be absorbed.

To illustrate the use of these gain–bandwidth plots, it is assumed that an input matching network is to be synthesized and the time constant of the input port of the FET is found out to be 0.25. If a gain ripple of 0.3 dB is acceptable, then from Fig. 6(a), point $P$ on the optimum curve can absorb the reactive element of the input port of the FET. The gain reduction is 1.01 dB in this case. On the other hand, if an input matching network is desired for a FET with more strict input gain–bandwidth limitations,

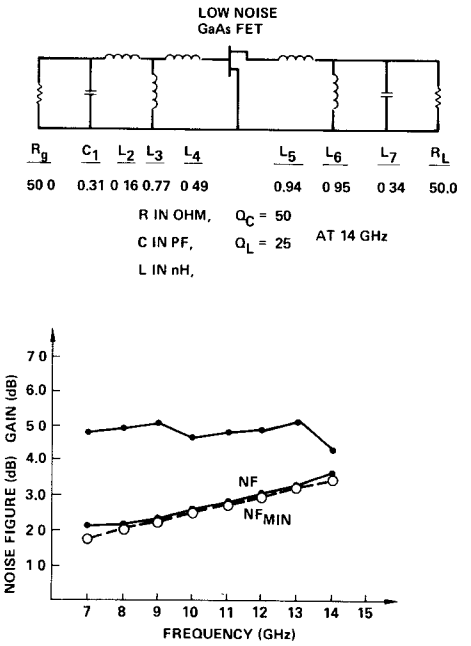


Fig. 7. Amplifier design, gain response, and noise figure of the low-noise amplifier using Hughes GaAs MESFET.

TABLE I
MEASURED $S$-PARAMETERS OF THE 0.5-$\mu$m GATE GaAs MESFET BIASED AT $V_D = 3$ V AND $I_D = 12$ mA

| FREQ. (GHz) | S11 MAG | S11 <ANG | S12 MAG | S12 <ANG | S21 MAG | S21 <ANG | S22 MAG | S22 <ANG |
|---|---|---|---|---|---|---|---|---|
| 7.00 | 0.888 | -57.677 | 0.063 | 61.479 | 1.254 | 115.379 | 0.764 | -40.284 |
| 8.00 | 0.828 | -67.075 | 0.064 | 54.445 | 1.147 | 104.645 | 0.727 | -47.946 |
| 9.00 | 0.817 | -72.691 | 0.056 | 56.424 | 1.118 | 99.724 | 0.769 | -49.660 |
| 10.00 | 0.812 | -80.151 | 0.067 | 54.262 | 1.052 | 92.062 | 0.773 | -53.840 |
| 11.00 | 0.819 | -84.816 | 0.068 | 55.187 | 1.029 | 87.187 | 0.777 | -58.916 |
| 12.00 | 0.815 | -88.303 | 0.068 | 54.049 | 0.991 | 79.249 | 0.787 | -62.362 |
| 13.00 | 0.775 | -93.012 | 0.073 | 55.581 | 1.006 | 74.181 | 0.750 | -70.123 |
| 14.00 | 0.732 | -100.767 | 0.070 | 51.608 | 0.925 | 62.308 | 0.777 | -80.259 |

e.g., with a time constant of 0.14, then only point $Q$ in Fig. 6(a) can absorb the reactive element if the gain ripple is kept at 0.3 dB. The gain reduction is increased to 2 dB in order to match this FET. A higher gain level can still be used if the gain ripple is larger. For example, point $R$ in Fig. 6(a) has 0.4-dB gain ripple, but a higher gain of $-1.9$ dB can also absorb the reactive element of the FET.

It may be noted that point $S$ in Fig. 6(a) has the same reactive element absorption capability as point $P$ but with a smaller gain ripple of 0.05 dB. Therefore, point $S$ is more desirable as long as the gain–bandwidth limitation is the only consideration. But sometimes point $P$ is preferred when the impedance transformation ratio between the two ends of the matching network is also considered.

## V. Design Example

A Hughes 0.5-$\mu$m low-noise GaAs MESFET [13] is used as a broad-band low-noise amplifier design example covering the octave frequency band from 7 to 14 GHz. The $S$-parameters of this FET are shown in Table I. Based on

the input $RC$-series model ($R_{in} = 12.23\ \Omega$, $C_{in} = 0.27$ pF) of the FET and the measured noise figure of 2.53 dB at 10 GHz, the simplified noise model developed by Podell, Ku, and Liu [12] can be used to predict the noise figure and the optimum source impedance at each frequency. The calculation shows that in order to obtain a minimum noise figure of 3.43 dB at 18 GHz, a $RC$-parallel equivalent circuit with $R_{in} = 59.56\ \Omega$ and $C_{in} = 0.25$ pF has to be matched at the input side. A lumped lossy input matching network with $n = 4$, flat gain, a 0.78-dB gain reduction, and a 0.05-dB gain ripple covering 2:1 band is synthesized through LUMSYN. The output model of the circuit cascading input noise matching network and the FET is calculated to be a $RC$-parallel circuit with $R_0 = 321.31\ \Omega$ and $C_0 = 0.17$ pF. A lumped lossy matching network is then synthesized to absorb this output model. The output matching network has $n = 4$, flat gain, 1.57-dB gain reduction, 0.2-dB gain ripple, and covers 2:1 band. Some optimization iterations are then used to make the overall gain response flatter. The final amplifier design and its gain response together with the noise figure are shown in Fig. 7. Note that the lumped inductors in the matching network are assumed to have $Q$'s of 25 while capacitors have $Q$'s of 50 to 14 GHz.

## VI. Conclusion

Systematic computer-aided synthesis techniques for matching networks in MMIC's have been developed and presented in this paper. The synthesis of the lumped matching network can incorporate the arbitrary loss factor associated with each reactive element and provide a very good initial design for a practical MMIC network. The application of this synthesis technique in the low-noise broad-band GaAs MESFET amplifier design is also presented to illustrate the general applicability of our computer-aided synthesis technique for broad-band GaAs MESFET MMIC amplifiers.

## References


[1] R. A. Pucel, "Design considerations for monolithic microwave circuits," *IEEE Trans. Microwave Theory Tech.*, vol. MTT-29, pp. 513–534, June 1981.

[2] W. R. Wisseman, "GaAs technology in the 80's," *Microwave J.*, vol. 24, pp. 16–18, Mar. 1981.

[3] W. C. Petersen, "Analytic and computer aided design techniques for bipolar and FET transistor amplifiers," Ph.D. thesis, Cornell Univ., Jan. 1976.

[4] A. Ralston, *Mathematical Method for Digital Computers*. New York: Wiley, 1966.

[5] K. M. Brown, "A quadratically convergent Newton-like method based upon Gaussian elimination," *SIAM J. Numerical Anal.*, vol. 6, pp. 560–569, Dec. 1969.

[6] D. W. Marquardt, "An algorithm for least-squares estimation of nonlinear parameters," *SIAM J. Appl. Math.*, vol. 11, pp. 431–441, 1963.

[7] T. J. Aird and J. R. Rice, "Systematic search in high dimensional sets," *SIAM J. Numerical Anal.*, vol. 14, pp. 296–312, Apr. 1977.

[8] H. W. Bode, *Network Analysis and Feedback Amplifier Design*. New York: Van Nostrand, 1945.

[9] R. M. Fano, "Theoretical limitations on the broadband matching of arbitrary impedances," *J. Franklin Inst.*, vol. 249, pp. 57–83, Jan. 1950; pp. 139–155, Feb. 1950.

[10] D. C. Youla, "A new theory of broadband matching," *IEEE Trans. Circuits Theory*, vol. CT-11, pp. 30–50, Mar. 1964.

[11] W. H. Ku and W. C. Petersen, "Optimum gain–bandwidth limitations of transistor amplifiers as reactively constrained active two-port networks," *IEEE Trans. Circuits Syst.*, vol. CAS-22, pp. 523–533, June 1975.

[12] A. Podell, W. H. Ku, and L. Liu, "Simplified noise model and design of broadband low-noise MESFET amplifiers," in *Proc. 7th Biennial Conf. on Active Microwave Semiconductor Devices and Circuits*, (Cornell University), Aug. 1979, pp. 429–443.

[13] D. W. Maki, R. Esfandiari, H. Yamasaki, M. Siracusa, and W. F. Marx, "A monolithic low noise amplifier," in *Proc. 8th Biennial Conf. on Active Microwave Semiconductor Devices and Circuits*, (Cornell University), pp. 27–36, Aug. 1981.


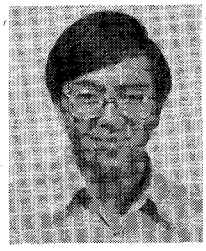


**Louis C. T. Liu** (S'77–M'81) was born in Taipei, Taiwan, Republic of China, on April 24, 1952. He received the B.S. degree in electrical engineering from the National Taiwan University, Taipei, in 1974, and the M.S. and Ph.D. degrees in electrical engineering from Cornell University, Ithaca, New York, in 1978 and 1981, respectively.

While at Cornell University, he worked as a graduate research assistant in the field of microwave broad-band circuit synthesis and design with applications in both low-noise and high-power GaAs MESFET amplifiers, as well as monolithic microwave integrated circuits. In May 1981, he joined the Torrance Research Center of Hughes Aircraft Company, Torrance, CA, where he has been involved in the design and development of GaAs monolithic microwave integrated circuits. His current work is focused on the design of various monolithic low-noise amplifiers and receive modules operating from *X*-band to *Ka*-band.



**Walter H. Ku** (S'56–M'62) received the B.S. degree (with Honors) from the Moore School of Electrical Engineering of the University of Pennsylvania, Philadelphia, and the M.S. and Ph.D. degrees from the Polytechnic Institute of Brooklyn, NY, all in electrical engineering. From 1957 to 1960, he held a Research Fellowship at the Polytechnic Institute of Brooklyn.

From 1960 to 1962, he was on the research staff of the Microwave Research Institute (MRI) of the Polytechnic Institute of Brooklyn. During the summers of 1956 and 1958, he was employed by IBM and Vitro Electronics Corporation. From 1962 to 1969, he was with the Applied Research Laboratory of the Sylvania Electronic Systems as an Engineering Specialist, a Senior Engineering Specialist, and a Senior Scientist. He joined the faculty of the School of Electrical Engineering of Cornell University in 1969 and is presently Professor of Electrical Engineering. In 1973–74, he was on leave from Cornell University and was a Visiting Associate Professor at the Department of Electrical Engineering and Computer Sciences of the University of California, Berkeley. For the 1977 academic year, he was on sabbatical leave from Cornell University and was the first occupant of the Naval Electronic Systems Command (NAVELEX) Research Chair Professorship at the Naval Postgraduate School, Monterey, CA. As the NAVELEX Research Chair holder, he was an Expert Consultant to NAVELEX and the Naval Research Laboratory (NRL), Washington, DC. Dr. Ku is currently a Distinguished Visiting Professor at the Department of Electrical Engineering and Computer Sciences of the University of California, San Diego, La Jolla, CA. Dr. Ku has served over the years as a consultant to GT&E-Sylvania Electronic Systems, Air Force RADC, Honeywell Radiation Center, TRW, Planar Microwave International Corporation (PLAMIC), Microwave Semiconductor Corporation (MSC), Rockwell International Science Center, and COMSAT. He is presently a Consultant to the Department of Defense on several microwave monolithic programs, the DARPA Space-Based Radar (SBR) Module Programs, and the OUSDRE VHSIC Program.

His current research interests are in the area of design and fabrication of submicron gate-length MOS and GaAs FET's and GaAlAs/GaAs heterojunction bipolar transistor, monolithic microwave and millimeter-wave devices and IC's, phased array modules and sampled analog and digital signal processing (DSP) techniques, and VLSI/VHSIC chip architectures and gigabit logic. His research has also been involved in adaptive signal processing and efficient implementations of spectral estimation algorithms. He was an Associate Editor of the IEEE TRANSACTIONS ON

CIRCUITS AND SYSTEMS, and was a Co-Chairman of the Technical Committee on Optical, Microwave and Acoustical Circuits (OMAC) of the IEEE Circuits and Systems Society and a Co-Chairman of the Technical Committee on Microwave Computer-Aided Design (MTT Group *1*) of the IEEE Microwave Theory and Techniques Society. He is an Associate Editor of the *Journal of Franklin Institute*.

Dr. Ku is a member of Eta Kappa Ku, Tau Beta Pi, Sigma Tau, Phi Tau Phi, and Sigma Xi. He is a Faculty Member of the National Research and Resource Facility for Submicron Structures (NRRFSS), and has been recently elected a Member of the Executive Committee of the new Semiconductor Research Corporation (SRC) Center of Excellence on Microstructure and Technology established at Cornell University.

# 2–20-GHz GaAs Traveling-Wave Power Amplifier

YALCIN AYASLI, MEMBER, IEEE, LEONARD D. REYNOLDS, ROBERT L. MOZZI, AND LARRY K. HANES

***Abstract*—Power amplification in FET traveling-wave amplifiers is examined, and the mechanisms which limit power capability of the amplifier are identified. Design considerations for power amplification are discussed. A novel single-stage and two-stage monolithic GaAs traveling-wave power amplifier with over 250-mW power output in the 2–20-GHz frequency range is described.**

## I. INTRODUCTION

THE WIDE BANDWIDTH capability of distributed or traveling-wave amplifiers is well known [1]–[3]. Traveling-wave amplification by adding the transconductance of several FET's without paralleling their input or output capacitances looks very promising for achieving wide-band microwave amplification. Already 2–20-GHz decade band amplification with 30-dB gain has been reported with GaAs FET's in monolithic form [4]. The relative insensitivity of the amplifier performance with respect to transistor and circuit parameter variations, good input and output match, and stable operation of these devices makes them very attractive for future commercial and military applications. Because of these potential applications, the power performance of the device is also of great interest; however, to our knowledge this problem has not yet been addressed in the literature.

This work discusses the power-limiting mechanisms in a GaAs FET traveling-wave amplifier and describes a new circuit approach which decreases the effect of some of these limiting mechanisms. In particular, design and performance of a 2–20-GHz power amplifier are presented.

Manuscript received June 14, 1983; revised December 15, 1983. This work was supported in part by the Air Force Wright Aeronautical Laboratories, Avionics Laboratory, Air Force Systems Command, U.S. Air Force, Wright-Patterson Air Force Base, OH.

The authors are with Raytheon Research Division, 131 Spring St., Lexington, MA 02173.

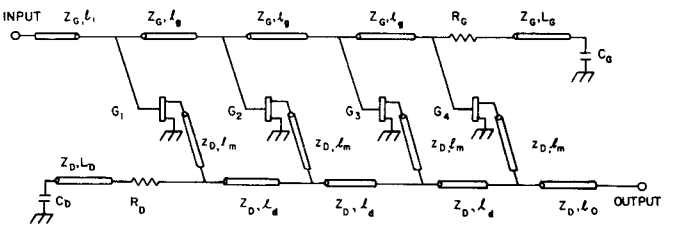


Fig. 1. Schematic representation of a four-cell FET traveling-wave preamplifier.

## II. TRAVELING-WAVE POWER AMPLIFICATION CONSIDERATIONS

Schematic representation of a four-cell FET traveling-wave amplifier is shown in Fig. 1. The design considerations and microwave performance of such an amplifier with GaAs MESFET's as active devices have been described in our earlier paper [5], where it was shown that when drain losses are small compared with gate-line losses, the small-signal gain expression for the amplifier can be written approximately as

$$G = \frac{g_m^2 n^2 Z_0^2}{4}\left(1 - \frac{\alpha_g l_g n}{2}\right)^2 \tag{1}$$

where

$g_m$ transconductance per FET,
$n$ number of FET's,
$Z_0$ input and output characteristic impedance,
$\alpha_g$ effective gate-line attenuation per unit length,
$l_g$ length of gate transmission line per unit cell.

This expression is derived using simplified circuit and device models. As such, it is not intended to be used as a design equation. However, despite its simplicity, (1) is very

0018-9480/84/0300-0290$01.00 ©1984 IEEE